Isolation and Characterization of Dermal Lymphatic and Blood Endothelial Cells Reveal Stable and Functionally Specialized Cell Lineages

Ernst Kriehuber,[1] Silvana Breiteneder-Geleff,[2] Marion Groeger,[3] Afschin Soleiman,[2] Sebastian F. Schoppmann,[2] Georg Stingl,[1] Dontscho Kerjaschki,[2,5] and Dieter Maurer[1,4]

[1]*Division of Immunology, Allergy and Infectious Diseases, Department of Dermatology,* [2]*Department of Pathology, and* [3]*Division of General Dermatology, University of Vienna Medical School, Allgemeines Krankenhaus, A-1090 Vienna, Austria*

[4]*Center of Molecular Medicine of the Austrian Academy of Sciences, A-1090 Vienna, Austria*

[5]*Center of Excellence for Clinical and Experimental Oncology, AUH-Vienna, A-1090 Vienna, Austria*

Abstract

A plexus of lymphatic vessels guides interstitial fluid, passenger leukocytes, and tumor cells toward regional lymph nodes. Microvascular endothelial cells (ECs) of lymph channels (LECs) are difficult to distinguish from those of blood vessels (BECs) because both express a similar set of markers, such as CD31, CD34, podocalyxin, von Willebrand factor (vWF), etc. Analysis of the specific properties of LECs was hampered so far by lack of tools to isolate LECs. Recently, the 38-kD mucoprotein podoplanin was found to be expressed by microvascular LECs but not BECs in vivo. Here we isolated for the first time podoplanin$^+$ LECs and podoplanin$^-$ BECs from dermal cell suspensions by multicolor flow cytometry. Both EC types were propagated and stably expressed VE-cadherin, CD31, and vWF. Molecules selectively displayed by LECs in vivo, i.e., podoplanin, the hyaluronate receptor LYVE-1, and the vascular endothelial cell growth factor (VEGF)-C receptor, fms-like tyrosine kinase 4 (Flt-4)/VEGFR-3, were strongly expressed by expanded LECs, but not BECs. Conversely, BECs but not LECs expressed VEGF-C. LECs as well as BECs formed junctional contacts with similar molecular composition and ultrastructural features. Nevertheless, the two EC types assembled in vitro in vascular tubes in a strictly homotypic fashion. This EC specialization extends to the secretion of biologically relevant chemotactic factors: LECs, but not BECs, constitutively secrete the CC chemokine receptor (CCR)7 ligand secondary lymphoid tissue chemokine (SLC)/CCL21 at their basal side, while both subsets, upon activation, release macrophage inflammatory protein (MIP)-3α/CCL20 apically. These results demonstrate that LECs and BECs constitute stable and specialized EC lineages equipped with the potential to navigate leukocytes and, perhaps also, tumor cells into and out of the tissues.

Key words: endothelial cell lineages • podoplanin • endothelial cell tube formation • vascular endothelial cell growth factors • chemokines

Introduction

The microvasculature of the blood and lymphatic systems form anatomically distinct, nonanastomozing networks (1–3). However, they constitute a functional continuum, in which the task of blood vessels is to import fluids, dissolved proteins, and cells into interstitial spaces, while the lymphatics provide the complementary exit route. Presumably, endothelial cells (ECs)* of blood vessels (BECs) and of lymphatic channels (LECs) are specialized and adapted for distinct functions. It would be a major achievement, if the dif-

E. Kriehuber and S. Breiteneder-Geleff contributed equally to this work.

Address correspondence to Dr. Dontscho Kerjaschki, Department of Pathology, University of Vienna, Waehringer Guertel 18-20, A-1090 Vienna, Austria. Phone: 43-1-40400-5176; Fax: 43-1-40400 5193; E-mail: Dontscho.Kerjaschki@akh-wien.ac.at

**Abbreviations used in this paper:* BEC, blood vessel EC; CCR, CC chemokine receptor; DC, dendritic cell; EC, endothelial cell; Flt-4, fms-like tyrosine kinase 4; LEC, lymphatic EC; MIP, macrophage inflammatory protein; nt, nucleotide(s); PFA, paraformaldehyde; SLC, secondary lymphoid tissue chemokine; UEA I, *Ulex europeaus* agglutinin I; VEGF, vascular endothelial cell growth factor; vWF, von Willebrand factor; WP, Weibel-Palade.

ferent molecular make-ups of LECs and BECs could be assembled into a catalog of gene expression and function. This could provide the basis for the understanding of the molecular mechanisms of complex processes such as transport of APCs and metastatic spread of tumor cells into regional lymph nodes. To unravel these functional differences, isolation and culturing of LECs and BECs are required. While isolated BECs are available from several tissues, this is not the case for LECs and, therefore, our present knowledge about the molecular regulation of LEC function is rudimentary, at best.

In this study we capitalized on our recent observation that the 38-kD transmembrane mucoprotein podoplanin is expressed by LECs in various human tissues (4), and serves as specific, protease-resistant marker for the isolation of pure LEC and BEC populations. This has opened the possibility to determine some of the characteristic features of LECs, to analyze their lineage fidelity and functional repertoire, with special reference to the production of factors that govern leukocyte trafficking in vivo.

Materials and Methods

Abs. Primary nonconjugated mouse mAbs used were anti–VE-cadherin (Immunotech), -CD31 (Ancell), -CD44 (Bender MedSystems), -CD45 (Becton Dickinson), and Pal-E (Harlan Sera-Lab). FITC-conjugated Abs included anti-CD34 (Becton Dickinson), sheep anti-von Willebrand factor (vWF; Serotec), goat anti–mouse $F(ab')_2$ (Jackson ImmunoResearch Laboratories), and goat anti–rabbit $F(ab')_2$ (Immunotech). PE- and RPE-Cy5–conjugated mAbs were anti-CD34 (Becton Dickinson) and anti-CD45 (Serotec). Biotinylated reagents were anti-CD31 (Ancell) and *Ulex europeaus* agglutinin I (UEA I; Vector Laboratories). The binding of biotinylated reagents was revealed by PE-conjugated streptavidin (Becton Dickinson). Preimmune goat IgG was obtained from Sigma-Aldrich. Goat anti–rabbit IgG conjugated to 10-nm gold particles was purchased from Amersham Pharmacia Biotech. Rabbit anti-podoplanin IgG was generated and characterized as described (4), using recombinant human podoplanin as the antigen. Human podoplanin (sequence data are available from GenBank/EMBL/DDBJ under accession no. AF390106) was expressed in *Escherichia coli*, and purified by FPLC (reference 4, and unpublished data). Rabbits were initially immunized with 50 mg antigen in CFA, followed by two boosts, and antisera were affinity-purified on nitrocellulose immobilized podoplanin, as described (4). Rabbit anti-caveolin was obtained from Becton Dickinson.

Dermal Cell Suspensions. Dermatomed 0.8-mm split-thickness skin was obtained from adult healthy individuals undergoing elective surgery (breast reduction and abdominoplasty). Dermal sheets were prepared by incubation of split-thickness skin with dispase (50 U/ml; Collaborative Medical Products) for 30 min at 37°C, and subsequent removal of the epidermis. Dermal cells were released from the tissue by scraping. Cells were pelleted, resuspended in EC growth medium MV (PromoCell), and either seeded on fibronectin (10 μg/ml; Life Technologies)-coated dishes for in vitro expansion, or subjected to immunostaining as described below.

Immunoisolation of EC Subsets from Dermal Cell Suspensions (Approach A). The procedures below are for the isolation of podoplanin$^+$ and podoplanin$^-$ microvascular ECs from freshly prepared dermal cell suspensions (approach A). Dermal cells were incubated for 7 min at 37°C in trypsin/EDTA (Life Technologies). Cell pellets were resuspended in ice-cold PBS/2 mM EDTA/0.5% BSA (Sigma-Aldrich), and the resulting cell suspension was filtered through a sterile sieve with 200 μm mesh-size, to remove fibers and cell aggregates. Cells were adjusted to 10^7 cells/ml in EC growth medium MV, supplemented with 10 μg/ml normal goat IgG, and exposed simultaneously to rabbit anti-podoplanin serum (final concentration: 1:100), anti–CD34-PE and anti–CD45-RPE-Cy5 (2 μg/ml each), or to appropriate control Abs for 45 min on ice. After two washes, the binding of rabbit Abs was revealed by incubation with goat anti–mouse $F(ab')_2$ FITC (10 μg/ml for 30 min). The staining procedure did not interfere with cell viability, as determined by trypan blue exclusion (data not shown). Cells were washed, resuspended in cold PBS/2 mM EDTA/0.5% BSA, and subjected to flow cytometry analysis. Podoplanin$^+$CD34$^+$CD45$^-$ and podoplanin$^-$CD34$^+$CD45$^-$ EC subsets were sorted on a FACStar$^{PLUS™}$ flow cytometer (Becton Dickinson). The purity of the sorted cell fractions was analyzed on a FACScan™ (Becton Dickinson) and always exceeded 98%. 0.5×10^6 sorted cells/ml were cultured on fibronectin (10 μg/ml)-coated 96-well flat bottom plates (Becton Dickinson) in EC growth medium MV.

Isolation of Subsets from Bulk Cultures of Dermal ECs (Approach B). Freshly isolated dermal cell suspensions were cultured in EC growth medium MV until confluent monolayers were formed. Loosely attached cells were discarded and adherent cells harvested by trypsinization as described above. 10^8 streptavidin-conjugated paramagnetic beads (Dynal) were coated with 10 μg biotinylated UEA I. Dermal cells (10^7/ml) were incubated with UEA I–coated beads (bead/cell ratio, 1:4), and ECs attached to the beads were isolated using a magnet. UEA I$^+$ ECs were passaged twice, harvested by trypsinization, and exposed simultaneously to anti-podoplanin (1:100), anti-CD31–biotin, and anti-CD45–RPE-Cy5 Abs (2 μg/ml each) followed by streptavidin-PE and goat anti–mouse $F(ab')_2$ FITC. ECs were sorted into podoplanin$^+$CD31$^+$CD45$^-$ and podoplanin$^-$CD31$^+$CD45$^-$ subsets on a FACStar$^{PLUS™}$.

Flow Cytometry Analysis of Blood Vessel and Lymphatic ECs. Plastic-adherent EC subsets were washed twice in ice-cold PBS/2 mM EDTA/0.5% BSA and then detached from the plates by gentle pipetting. Cells obtained were incubated with the indicated primary Abs or with appropriate control Abs for 60 min on ice. Primary Abs were detected by incubation with goat anti–mouse $F(ab')_2$ FITC or goat anti–rabbit $F(ab')_2$ FITC (2 μg/ml each). To reveal cytoplasmic vWF expression, cells were fixed and permeabilized before the immunostaining procedure, using a kit according to the manufacturer's instructions (Fix&Perm; An der Grub). Cellular fluorescence was analyzed on a FACScan™ flow cytometer.

Double Immunofluorescence of Tissue Sections and Cultured ECs. 5-μm cryosections were cut from skin specimens of healthy human donors, mounted onto glass slides, air-dried, and rehydrated in HBSS. ECs were cultured on fibronectin-coated LabTek chamber glass slides (Nunc). Cells were fixed in 4% paraformaldehyde (PFA)/PBS for 20 min. Slide-bound ECs or skin sections were incubated for 30 min in blocking solution (5 mM $CaCl_2$, 1% BSA, and 10 μg/ml goat IgG in HBSS) before their simultaneous exposure to rabbit anti-podoplanin and the indicated mAbs overnight. Binding of the primary polyclonal and monoclonal Abs was revealed by subsequent incubation with goat anti–mouse TRITC and goat anti–rabbit FITC (5 μg/ml each). Samples were mounted in Vectorshield medium (Vector Labora-

tories) and were analyzed by laser scanning microscopy (LSM 410; ZEISS).

Immunoelectron Microscopy. UEA I^+ ECs were isolated as described above and expanded through five culture passages. ECs were harvested, seeded onto fibronectin-coated glass coverslips, and cultured for the indicated time periods. Then, coverslip-bound ECs were fixed in 4% PFA/PBS for 6 h at 20°C, and processed for preembedding anti-podoplanin immunogold labeling, as described (4). Ultra-thin sections were examined under a JEOL 100 CX electron microscope (JEOL).

Immunoblotting. ECs were grown to 80% confluence, lysed in reducing SDS sample buffer, and proteins were electrophoresed by 5–15% gradient or 6% straight SDS-PAGE and transferred onto nitrocellulose membranes (Bio-Rad Laboratories). Membranes were cut and strips were incubated with the following Abs: rabbit anti-podoplanin (final dilution 1:1,000), rabbit fms-like tyrosine kinase 4 (Flt-4) (C-terminus-reactive), -KDR, -Flt-1, -Tie-1, -Tie-2 (0.5 μg/ml each; Santa Cruz Laboratories, Inc.), or mouse anti-CD31 (0.5 μg/ml). Strips were washed, and binding of primary Abs was revealed as described previously (5).

Northern Blotting. Total RNA was extracted using Tri-Reagent (Molecular Research Center) according to the manufacturer's instructions. 20 μg of RNA were separated on 1% formaldehyde-agarose gels and transferred onto Zeta Probe nylon membranes (Bio-Rad Laboratories), and hybridized to the following ^{32}P-labeled cDNA fragments: podoplanin (nucleotides [nt] 136–653), LYVE-1 (nt 91–1054), Flt-4 (nt 554–1340), CD31 (nt 605–1397), vascular endothelial cell growth factor (VEGF)-C (nt 353–849), and β-actin (CLONTECH Laboratories, Inc.). Hybridization was performed at 65°C for 18 h. Then, membranes were washed twice in 5% SDS/20 mM Na_2HPO_4, pH 7.2, at 65°C for 30 min followed by two washes in 1% SDS/20 mM Na_2HPO_4, pH 7.2, at 60°C for 10 min, and exposed for 1 to 3 d to X-ray films.

Tube-forming Assay. Plastic-adherent ECs were labeled with 5(and 6)-([{4 chloromethyl}benzoyl] amino)tetramethylrhodamino (CMTMR) or with 5-chloromethylfluorescein diacetate (CMFDA) fluorescent cell trackers (100 nM; both from Molecular Probes) in HBSS for 15 min at 37°C. Free label was removed, cells were cultured for 12 h in EC growth medium, and detached from the plate by trypsin/EDTA. 24-well culture dishes were coated with 0.5 ml Matrigel (both from Becton Dickinson) per well on ice and gels were allowed to solidify for 60 min at 20°C. 2.5×10^5 CMTMR- or CMFDA-labeled ECs were seeded into individual Matrigel-coated wells and incubated for 24 h. Finally, cells were fixed in 4% PFA/HBSS for 30 min and samples were analyzed by confocal laser scanning microscopy. In some experiments equal numbers of prelabeled BECs and LECs were mixed 1:1, and then subjected to the tube-forming assay.

Cytokine Stimulation of Lymphatic and Blood Vessel ECs. ECs were grown to confluence in EC growth medium MV in 75-cm^2 culture flasks (Becton Dickinson), or onto 0.4-μm poresize Transwells™ inserted into individual wells of 24-well plates (Costar). Then, full medium was replaced by EGF- and hydrocortisone-deficient EC growth medium MV, and cells were cultured for 24 h to confluence. Plastic-adherent and Transwell™-bound ECs were washed twice and cells were cultured in the presence or absence of TNFα (100 U/ml) or IL-1β (0.1 ng/ml; both from R&D Systems). After 24 h, culture fluid from supernatant (from the upper and lower compartment in Transwell™ experiments) were harvested, and CCL19, CCL21, and CCL20 were measured by ELISA (vide infra).

Chemokine ELISA. 96-well ELISA plates (MaxiSorp™; Nunc) were coated with affinity-purified rabbit anti-CCL19, anti-CCL20, or anti-CCL21 Abs (0.2 μg/well each; all from PeproTech). 200 μl of EC-conditioned medium, fresh EC culture medium, or serial dilutions of recombinant CCL19, CCL20, or CCL21 (all from R&D Systems) were incubated at 4°C overnight. Plates were rinsed, and 0.2 μg of affinity-purified goat anti-CCL19, anti-CCL20, or anti-CCL21 (all from R&D Systems) were added to individual wells. After 45 min, plates were washed and incubated with biotin-conjugated rabbit anti–goat IgG, followed by incubation with alkaline phosphatase–conjugated streptavidin for 30 min (both from Sigma-Aldrich). CSPD alkaline phosphatase (Boehringer) was used as substrate, and signal intensities were measured on a luminometer (Berthold). All ELISA systems used were chemokine specific, and in control experiments 11 additional nontarget chemokines (CCL2, CCL3, CCL5, CCL7, CCL8, CCL13, CCL17, CCL22, CXCL12, CXCL13, CX3CL1; all from R&D Systems) failed to produce signals.

Results

Identification and Isolation of Dermal Lymphatic and Blood Vessel ECs. Dermal LECs, but not BECs, express podoplanin, while both EC subsets display CD34 (4; Fig. 1, A–C), and are consistently devoid of CD45 (6, 7). The only other dermal cell type known to display anti-CD34 reactivity is the fibrocyte that, however, expresses CD45 (8). Dermal cells were isolated by enzymatic digestion of dermal sheets, and labeled simultaneously with anti-

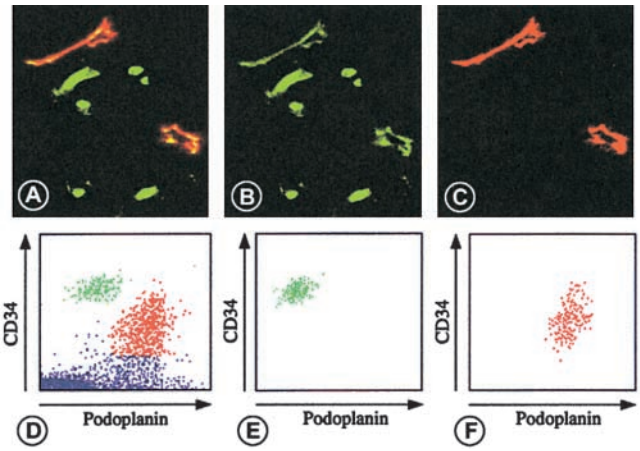

Figure 1. Identification of dermal BECs and LECs in cryostat sections of human skin (A–C), and isolation by FACS® (D–F). (A–C) Immunofluorescence double-labeling using Abs to podoplanin (TRITC, red), and CD34 (FITC, green). FITC and TRITC fluorescence images are shown in B and C. Panel A illustrates the double exposure with LECs (yellow-red) expressing both podoplanin and CD34. Microvascular tubes shown are ascending from the superficial vascular plexus (original magnification: ×400). (D–F) Isolation of BECs and LECs from dermal cell suspensions (approach A) prepared by enzymatic digestion. Cells were triple-labeled with anti-CD45 Cy5, anti-CD34-PE, and anti-podoplanin. $CD45^-$ cells were gated electronically, and $podoplanin^-/CD34^{high}$ (green, BECs) and $podoplanin^+/CD34^{low}$ ECs (red, LECs) were identified (D) and isolated (E and F) by FACS®. The purity of the two sorted EC subsets was >98%.

podoplanin, -CD34, and -CD45 Abs (Materials and Methods, approach A). After exclusion of $CD45^+$ cells, two EC populations with nonoverlapping immunophenotypes, i.e., podoplanin$^+$/$CD34^{low}$ = LECs (red dots; Fig. 1 D), and podoplanin$^-$/$CD34^{high}$ = BECs (green dots; Fig. 1 D) were clearly separated by flow cytometry. The minor podoplanin$^+$/$CD34^-$/$CD45^-$ cell population was presumably derived from large lymphatic vessels. By flow sorting, we obtained microvascular LECs and BECs at a purity of >98% (Fig. 1, E and F), without any intercalated culture step. As average yield from 15 independent experiments, $CD34^+$ ECs accounted for 5–10% of total dermal cells, and 70% therefrom were LECs and 30% BECs.

Separated microvascular EC populations were cultured in standard EGF-, hydrocortisone-, and bovine hypothalamic extract–conditioned EC growth medium (EC growth medium MV™). They formed cell clusters in the first days and, then, progressively confluent EC monolayers by day 7 to 10. Monolayers of LECs and BECs were indistinguishable by phase contrast microscopy (Fig. 2, A and B). Both EC populations were propagated for at least seven passages without altering their morphology.

Dermal Microvascular EC Bulk Cultures Contain Two Distinct EC Types that Differentially Express Podoplanin. As the number of LECs isolated directly from dermal cell suspensions was relatively low, we increased their yield by expanding freshly prepared dermal cells in EC growth medium, followed by enrichment of ECs by use of UEA I–conjugated magnetic beads, and two further passages of UEA I^+ ECs (Materials and Methods, approach B). Bulk cultured microvascular ECs, while of homogeneous appearance by light microscopy, contained two immunophenotypically distinct cell populations (Fig. 2 C). As shown in Fig. 2 C, islands of podoplanin$^+$ LECs are surrounded by podoplanin$^-$ BECs. For the FACS® sorting of preexpanded EC subsets, anti-CD31 instead of anti-CD34 mAbs were added to the immunolabeling mix as ECs downregulate CD34 during in vitro culture (reference 9, and data not shown). This amplification and cell sorting strategy yielded 10 times more ECs than direct isolation without intervening cell expansion. EC subsets isolated by approach B were identical to those generated by approach A; they also formed cell clusters and monolayers, and could be propagated for at least seven culture cycles.

Isolated and Cultured Lymphatic and Blood Vessel ECs Stably Express Cell Type–specific Markers. Expression of EC subset-defining and pan-EC antigens by LECs and BECs was determined at various passages (passage 1–7) by flow cytometry (EC subsets generated by approach A and B) as well as by Northern and/or Western blotting (EC

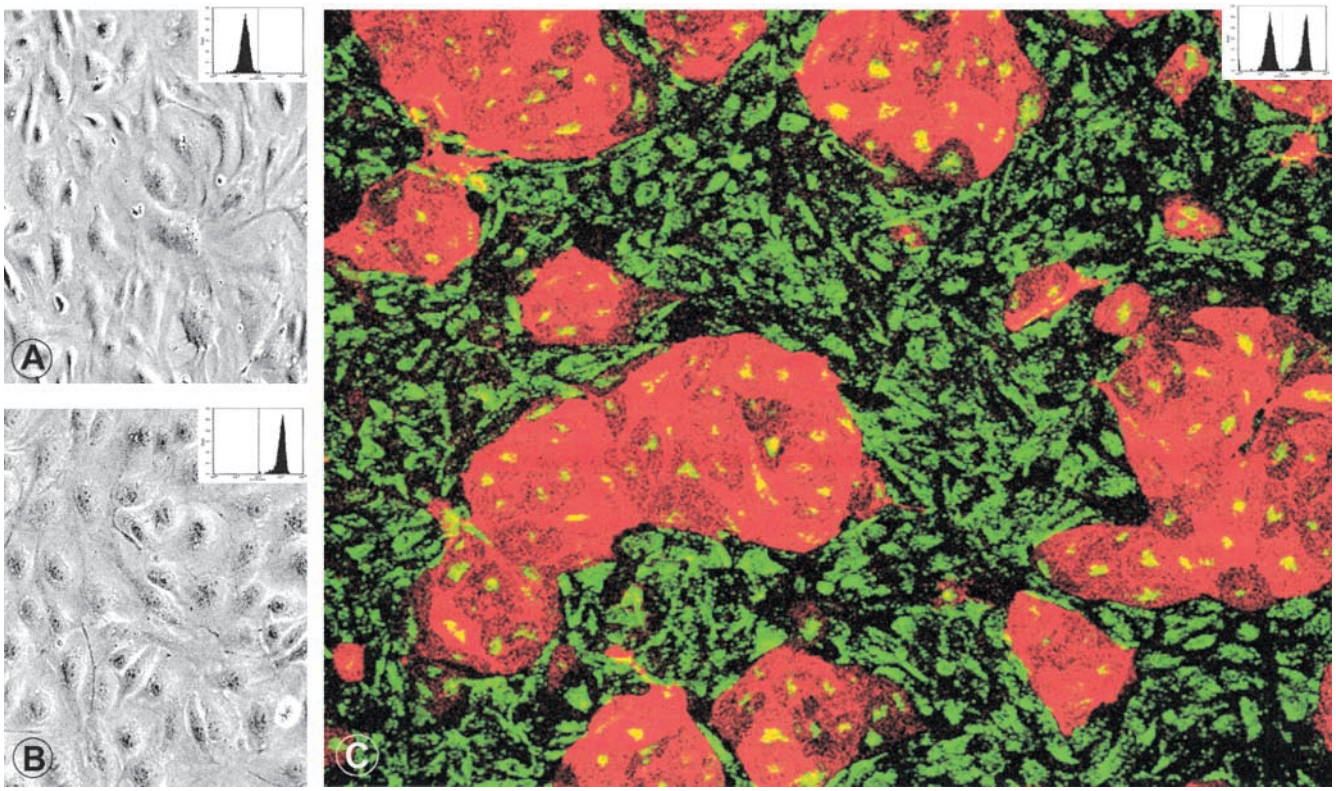

Figure 2. BECs and LECs cannot be distinguished by conventional light microscopy when grown separate (A, BECs; B, LECs). (C) In mixed cultures, immunolabeling with anti-podoplanin (TRITC, red) and anti-vWF (FITC, green) reveal multicellular islands of podoplanin$^+$/vWF$^+$ LECs surrounded by podoplanin$^-$/vWF$^+$ BECs. BECs express more vWF than LECs (see also Fig. 3 A). Original magnification in A and B: ×300; C: 250. To confirm their phenotypic stability, cultured LECs and BECs were harvested, labeled with anti-podoplanin IgG, and analyzed by FACS® (insets in A–C; dotted line denotes the cut-off for podoplanin positivity). Cultured BECs (A) were homogeneously podoplanin-negative, cultured LECs (B) exclusively podoplanin-positive, while the mixed EC population (C) contained both qualities.

subsets generated by approach B). Among the subset-restricted markers, LECs retained expression of 38 kD podoplanin, while BECs were consistently devoid of this moiety, irrespective of the purification strategy used (Fig. 3, A and C). Two species of podoplanin mRNA were observed by Northern blotting that presumably originate from alternative splicing (Fig. 3 B). Also the hyaluronate receptor LYVE-1 was selectively expressed by LECs, but not by BECs, similar to the in vivo situation (10; Fig. 3 B). Conversely, BECs, but not LECs, expressed the hyaluronate receptor CD44 and the PAL-E–reactive antigen (Fig. 3 A). PAL-E reactivity, however, was progressively downregulated after the second culture cycle. Of the characteristic pan-EC markers, both EC types maintained expression of CD31, VE-cadherin, and vWF (Fig. 2 C, and Fig. 3, A and B) and contained caveolae and Weibel-Palade (WP) bodies (Fig. 4). WP bodies were encountered more frequently and the WP body–associated antigen vWF was expressed at 10 times higher levels in cultured BECs than in LECs (Fig. 3 A). Expectedly, neither BECs nor LECs expressed CD45, smooth muscle actin, cytokeratins, and neurofilaments (data not shown).

Differential Expression of Vascular Growth Factors and Their Receptors by Lymphatic and Blood Vessel ECs. LECs and, to a much lesser extent, BECs express the VEGF-C/D receptor Flt-4 in vivo (1, 11–14). This expression profile is also recapitulated by in vitro propagated LECs and BECs. Cultured LECs, rather than BECs, pronouncedly express Flt-4 both at the mRNA and the protein level (Fig. 3, B and D). Anti–Flt-4 Ab-reactive 140-, 175-, and 195-kD bands presumably are differentially processed isoforms of the VEGF-C/D receptor (15), and were predominantly expressed by LECs (Fig. 3 C). The ~120–125-kD moieties that are expressed by LECs and in high levels by BECs (Fig. 3 D), correspond to proteolytic COOH-terminal fragments of Flt-4 (15). Contrary to the expression pattern of Flt-4, its ligand, VEGF-C, was produced by BECs, but not by LECs (Fig. 3 B). Two other VEGF receptors, Flt-1/VEGFR-1, and KDR/VEGFR-2, and the angiopoietin receptors Tie

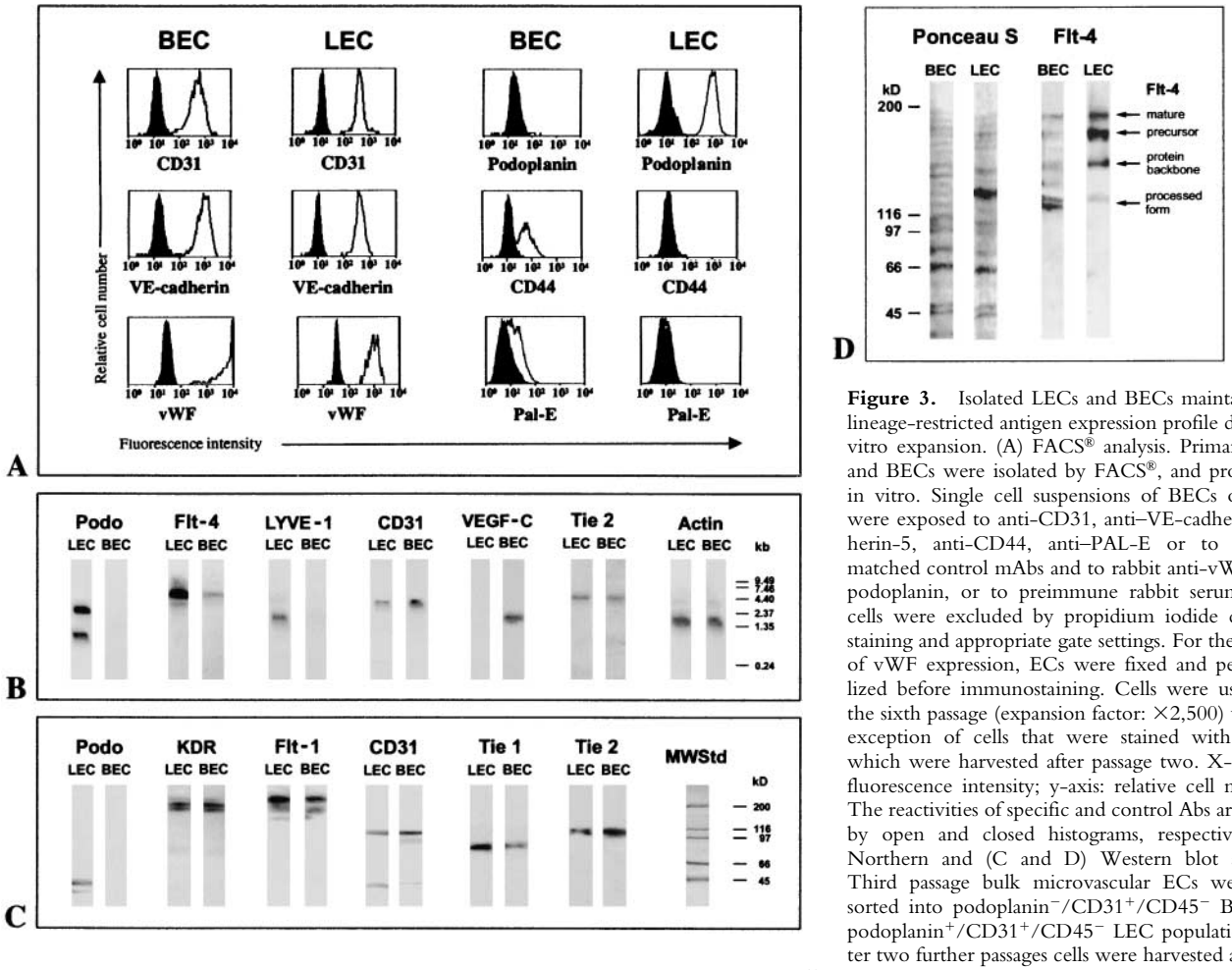

Figure 3. Isolated LECs and BECs maintain their lineage-restricted antigen expression profile during in vitro expansion. (A) FACS® analysis. Primary LECs and BECs were isolated by FACS®, and propagated in vitro. Single cell suspensions of BECs or LECs were exposed to anti-CD31, anti–VE-cadherin/cadherin-5, anti-CD44, anti–PAL-E or to isotype-matched control mAbs and to rabbit anti-vWF, anti-podoplanin, or to preimmune rabbit serum. Dead cells were excluded by propidium iodide counterstaining and appropriate gate settings. For the analysis of vWF expression, ECs were fixed and permeabilized before immunostaining. Cells were used after the sixth passage (expansion factor: ×2,500) with the exception of cells that were stained with PAL-E which were harvested after passage two. X-axis: log fluorescence intensity; y-axis: relative cell numbers. The reactivities of specific and control Abs are shown by open and closed histograms, respectively. (B) Northern and (C and D) Western blot analyses. Third passage bulk microvascular ECs were flow sorted into podoplanin$^-$/CD31$^+$/CD45$^-$ BEC and podoplanin$^+$/CD31$^+$/CD45$^-$ LEC populations. After two further passages cells were harvested and total cellular RNA and protein were isolated. (B) RNA transfers were sequentially hybridized with ^{32}P-labeled probes derived from the cDNA of podoplanin, Flt-4, LYVE-1, CD31, and VEGF-C. To ensure equal loading and transfer of RNA, membranes were finally hybridized with an actin probe. Positions of standards are shown on the right in kb. (C and D) Equal amounts of LEC- and BEC-derived proteins were blotted (D, left panel), membranes were probed with Abs against podoplanin, KDR, Flt-1, CD31, Tie-1, Tie-2 (C), or Flt-4 (D, right panel), and Ab reactivity was revealed by chemoluminescence. Positions of molecular weight markers are shown in kD.

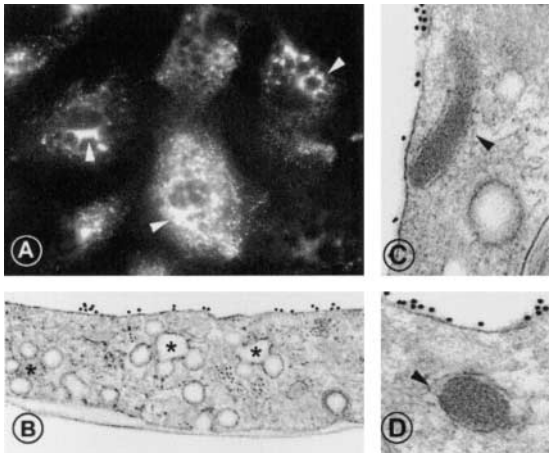

Figure 4. In vitro–cultured LECs contain caveolin and caveolae, and WP bodies. ECs were grown to confluence, fixed, labeled by indirect immunofluorescence for caveolin (A), or by a preembedding immunogold protocol for podoplanin (B). ECs express uniformly caveolin in a granular pattern (A) that corresponds in LECs to typical endothelial caveolae by electron microscopy (B). (C and D) Electron microscopy also reveals WP bodies in podoplanin-expressing LECs. Original magnification in A: ×700; B: ×12.000; C and D: ×45.000.

1 and Tie 2 were expressed at similar levels by BECs and LECs (Fig. 3, B and C).

Lymphatic ECs Form Continuous Homotypic Cell Junctions. When grown to confluence, ECs of both types sequester CD31 and VE-cadherin (Fig. 5, A–D), α- and β-catenin, and pp120^{cas} (data not shown) into sites of cell contacts. However, the marginal cell areas occupied by junctional contacts strikingly differed between LECs and BECs. Cell junctions between LECs were essentially linear, well demarcated, and equipped with a continuous but thin seam of VE-cadherin and CD31 (Fig. 5, A and C). In contrast, junctions formed by BECs were ruffled, often indented, and characterized by a broad overlap of the CD31- and VE-cadherin-bearing cell membranes (Fig. 5, B and D). By electron microscopy, junctional areas of LECs were equipped with adherens junctions (Fig. 5 E), gap junctions (Fig. 5 I), and tight junctions (Fig. 5, E–H). The latter presumably account for the virtual impermeability of LEC monolayers for exogenous chemokines, as probed with CCL19 (see below). Expectedly, adherens, gap, and tight junctions were observed in BECs (Fig. 5, J–L).

Lymphatic and Blood Vessel ECs Form Homotypic Associations and Vascular Tubes. When cultures containing BECs

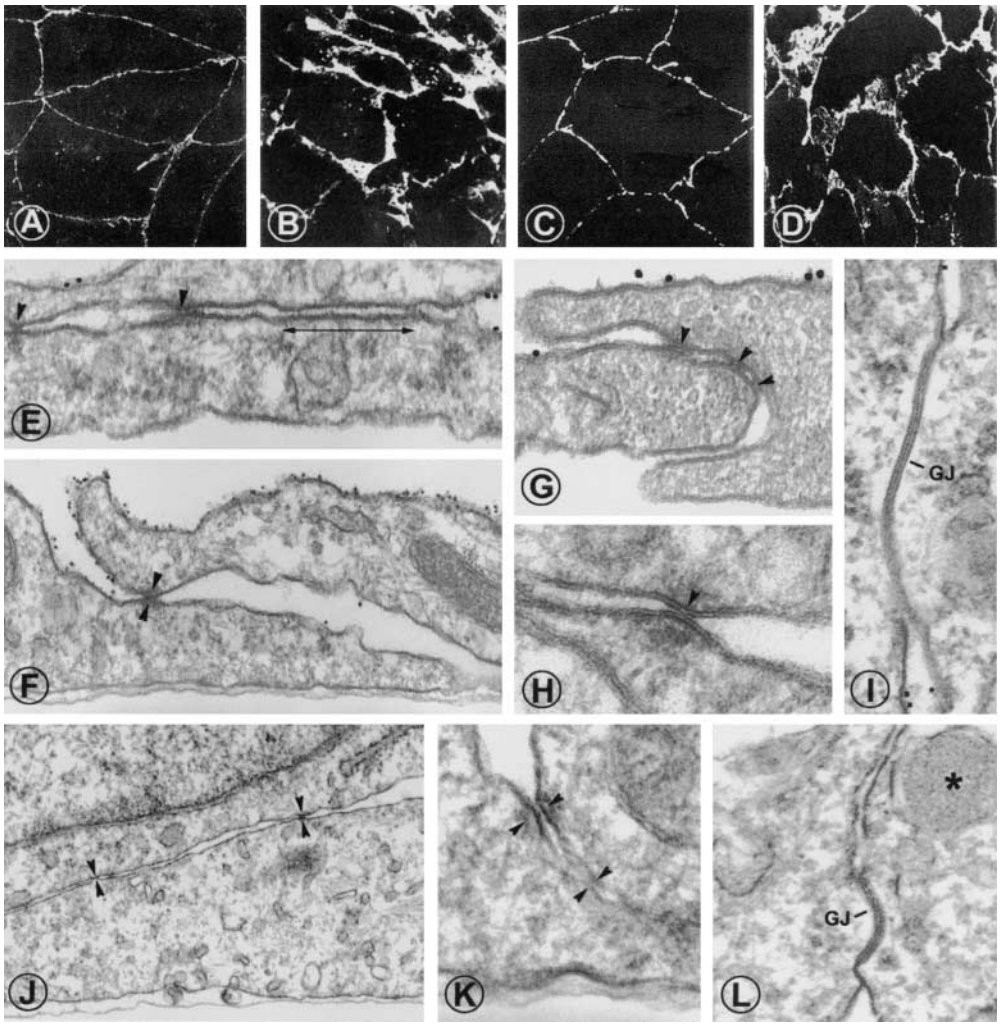

Figure 5. LECs form continuous homotypic cell junctions. (A–D) Cell contacts formed by LECs and those by BECs differ in the extent of junctional protein recruitment. Confluent LECs (A and C) and BECs (B and D) were fixed, and stained with anti-CD31 (A and B) or anti–VE-cadherin (C and D). LECs display a thin rim of CD31 and VE-cadherin in their junctional areas while BECs form ruffled, indented homotypic junctions with a broad overlap of the VE-cadherin- and CD31-bearing cell membranes. (E-I) Podoplanin$^+$ LECs were identified by 10 nm immunogold labeling. LECs form typical junctional complexes consisting of adherent junctions (E, double-headed arrow) and tight junctions (arrowheads in E–H). (I) Occasionally, gap junctions were observed. Similar junctional structures were also found on cultured, immunogold-negative BECs (J–L). Asterisk in L indicates a Weibel-Palade body, gap junctions are marked (GJ). Original magnification in A–D: ×700; E, G, I, K, and L: ×75.000; F and J: ×40.000; H: ×120.000.

and LECs were grown to confluence and replated for 12 h, islands of LECs formed that were surrounded by BECs (Fig. 2 C). EC bilayer formation occurred, when the culture was prolonged for 3 d after the cells had reached confluence. These consisted of plastic-adherent podoplanin$^-$/CD31$^+$ BECs and podoplanin$^+$/CD31$^+$ LECs on top (Fig. 6). In contrast, bilayer formation was never observed in monotypic cultures of FACS®-sorted LECs and BECs (Fig. 2, A and B).

Does this imply that LECs and BECs are capable of cell lineage–restricted cell recognition? To address this further, fluorescent dye–labeled BECs and LECs were subjected to tube-forming assays on Matrigel. Separately grown BECs and LECs formed tube-like structures (Fig. 7, A–D). LEC tubes were thin and rather uniform in diameter (Fig. 7, C and D), while BEC tubes appeared ragged with prominent nuclei (Fig. 7, A and B). Optical cross-sectioning of these EC structures by confocal microscopy revealed occasional lumen formation (not shown), as also documented by others previously (16). Thus, the EC cords formed on Matrigel are designated "tubes" in this study. When isolated BECs and LECs were labeled with red and green fluorescent dyes, respectively, mixed in a 1:1 ratio, and then cultured on Matrigel, tubes formed that consisted of one EC type only (Fig. 7, F–G). However, BEC tubes were closely associated with LEC tubes (Fig. 7 H).

Lymphatic and Blood Vessel ECs Produce Distinct Chemoattraction Signals. Confluent LECs and BECs were stimulated with TNFα or IL-1β or left nonstimulated. Chemokine production was assessed by ELISA. Secondary lymphoid tissue chemokine (SLC)/CCL21 was secreted by nonstimulated and, to a lesser extent, by cytokine-activated LECs but not by BECs or by other cell types (keratinocytes, fibroblasts, large blood vessel ECs) either in their resting or cytokine (TNFα, IL-1β)-activated state (Fig. 8 A). None of the above cell types released macrophage inflammatory protein (MIP)-3β/CCL19 whether activated or not (data not shown). In contrast to the LEC-restricted production of CCL21, LECs as well as BECs secreted MIP-3α/CCL20 (Fig. 7 B) and monocyte chemotactic protein (MCP-1)/CCL2 (data not shown) upon stimulation with IL-1β and TNF.

To investigate directional chemokine secretion, LECs were grown to confluence on 0.4-μm poresize Transwell™ filters inserted into 24-well tissue culture plates. Then, the culture medium above and below the membrane-bound EC monolayers was replaced by TNFα- or IL-1β supplemented or by nonsupplemented medium, and the amount of chemokines secreted into the apical and into the basolateral direction was measured after 24 h. To control for chemokine leakage through the LEC monolayer, CCL19, which is not secreted by ECs, was added into the upper compartment and the amount of CCL19 recovered in the upper and the lower compartment was measured. After 24 h, only 10% of totally recovered CCL19 was in the lower compartment. Thus, LECs formed a tight barrier that cannot be easily penetrated even by small molecules like chemokines (Fig. 8 D). As shown in Fig. 8 C, the vast majority of CCL20 was secreted in an apical/luminal direction.

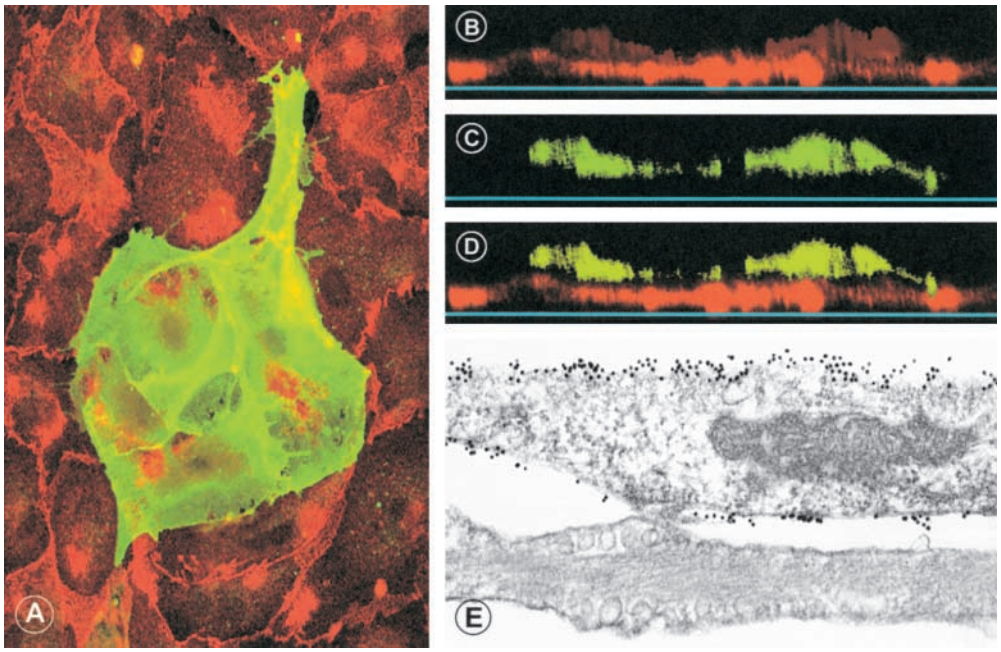

Figure 6. BECs and LECs form separate homotypic layers in mixed EC cultures. Mixed BECs and LECs were allowed to reach confluence and then were cultured for four additional days. (A–D) Cells were fixed and stained with anti-podoplanin Abs (FITC) and anti-CD31 (TRITC). In the double exposure shown in A, podoplanin$^+$/CD31$^+$ ECs (yellow) appear to cover the monolayer of podoplanin$^-$/CD31$^+$ ECs (red). In B–D, vertical optical sectioning by confocal microscopy directly shows that podoplanin$^+$/CD31$^+$/LECs (green; C and D) are positioned on top of podoplanin$^-$CD31$^+$ BECs (red; B and D). The blue line indicates the position of the culture dish. In E, EC bilayers were fixed and processed for anti-podoplanin immunogold labeling and vertical sections were analyzed by electron microscopy. LECs as identified by their intense labeling with 10-nm gold particles are found on top of nonlabeled BECs. Original magnification in A–D: ×1,000; E: ×40.000.

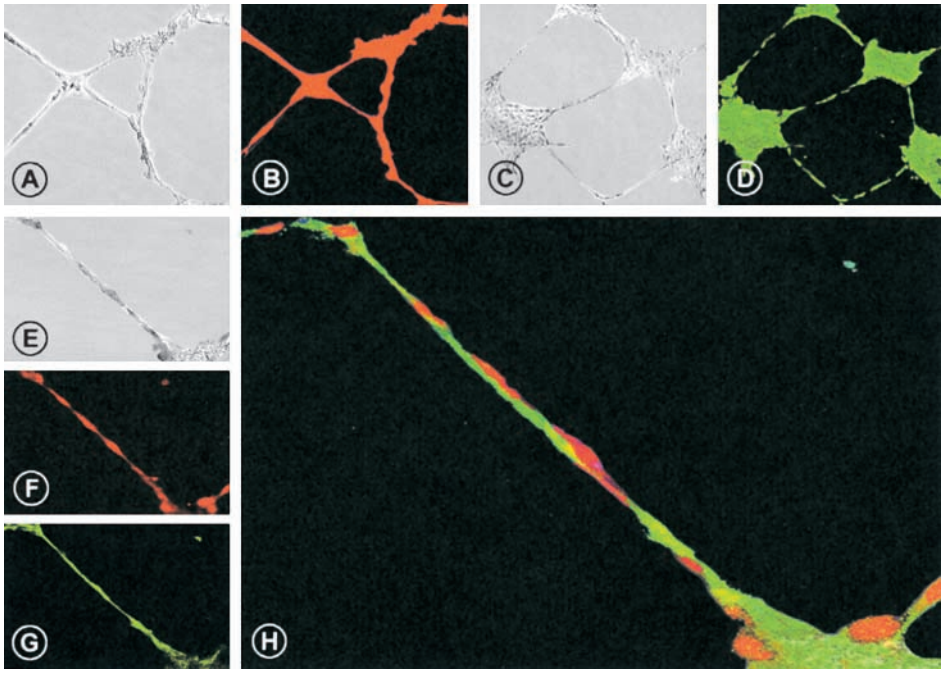

Figure 7. Lymph and blood ECs form independent capillary tubes that wind around each other. Flow-sorted primary BECs or LECs were expanded through six passages, harvested, and labeled with cell-permeant dyes emitting red and green fluorescence, respectively. Labeled BECs (A and B; red), LECs (C and D; green), or BECs and LECs mixed in a 1:1 ratio (E–H) were seeded onto Matrigel, cultured in EGF- and hydrocortisone-deficient medium for 24 h, fixed, and analyzed by confocal microscopy. A, C, and E are phase contrast images corresponding to the fluorescence images B (red), D (green), and F–H (green, red), respectively. F and G show the single red and single green fluorescence signals of the double exposure in H. (F and G) In mixed cultures, BECs and LECs form tubes that are built up by one EC subtype only. (H) Homotypic BEC and LEC tubes are closely juxtaposed in a double helical pattern. Original magnification in A–G: ×100; H: ×400.

In fact, 90% of secreted CCL20 and CCL2 were detected in the upper chamber (Fig. 8 C). In contrast, more than one third of SLC/CCL21 was secreted basolaterally (Fig. 8 C). It is of note that this secretion pattern was not changed by EC stimulation with proinflammatory cytokines (Fig. 8 C).

Discussion

EC biology and pathology owe their recent explosive growth, in part, to methods for cell isolation and propagation. Major advances in these fields, e.g., the identification of EC growth factors, chemokines and their receptors, the molecular understanding of how ECs interact with leukocytes and neoplastic cells, and others (17–20), were made by using cultured BECs as the research substrate. Due to the lack of specific marker molecules, the lymphatic EC system has received much less attention and the molecular mechanisms regulating lymphatic EC and vessel function have remained largely elusive. This situation may have also led to misconceptions about microvas-

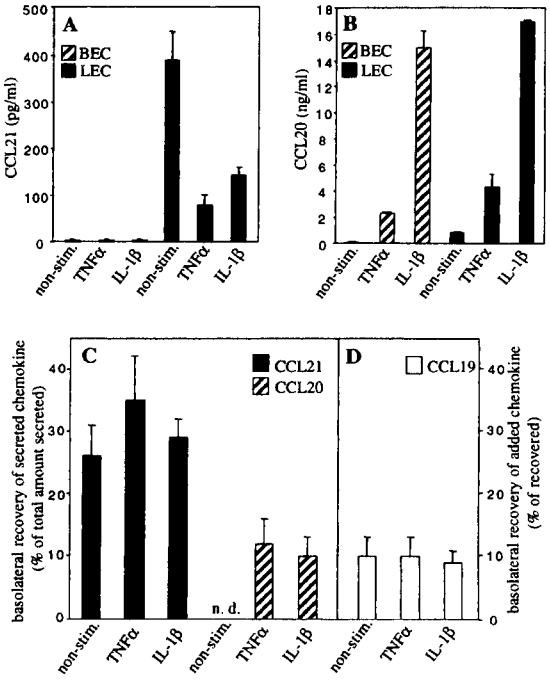

Figure 8. Chemokine secretion of isolated LECs and BECs. (A and B) LECs, but not BECs, secrete SLC/CCL21, but both EC types produce MIP-3α/CCL20 upon activation. EC subsets grown to confluence were exposed to EGF- and hydrocortisone-deficient medium (non-stim.) or to the same medium supplemented with TNFα or IL-1β. 24 h supernatants were analyzed by CCL21- (A) and CCL20-specific ELISAs (B). The concentrations of chemokines produced by BECs (hatched bars) and LECs (black bars) are shown (mean values (±SD) obtained in two independent experiments). (C) LECs secrete CCL21 but not CCL20 basolaterally. LECs grown to confluence on 0.4-μm poresize Transwell™ filters, were nonstimulated (non-stim.) or stimulated with TNFα- or IL-1β for 24 h. CCL21 (black bars) and CCL20 (hatched bars) secreted into the upper (apical) and the lower (basolateral) chamber of the Transwells™ were measured. The percentage of chemokine recovered from the lower chamber relative to the total amount of secreted chemokine (i.e., secreted into the upper and lower chamber) is shown. Mean values (±SD) obtained from triplicate cultures; n.d.; not done. (D) LEC monolayers form a tight barrier for exogenous CCL19 used as a tracer. To control for leakage of chemokines through the LEC monolayer, MIP-3β/CCL19 was added to the upper chamber. Data are given as the percentage of the amount of chemokine recovered from the lower chamber relative to the amount of chemokine retrieved from the upper and lower chamber. Approximately 80% of initially added CCL19 was recovered after 24 h. Mean values (±SD) obtained from triplicate cultures.

cular BEC gene expression and function since bona fide BECs may be "contaminated" by LECs. Until the not so distant past, lymphatic vessels were defined by the absence of erythrocytes from their lumen, and LECs, compared with BECs, by their less elaborate cell junctions and basement membranes as well as their low level expression of CD34 and vWF (6, 7). Recently, two glycoproteins were discovered that are selectively expressed in LECs, but not in BECs. These are the transmembrane protein podoplanin, originally found in glomerular podocytes (21), and a CD44-related hyaluronic acid receptor designated LYVE-1 (10). The expression pattern of these markers is conserved in rodents, as the podoplanin ortholog E11/T1 α in rat (22, 23), and the LYVE-1 ortholog in mice (24) are expressed by lymphatic but not blood ECs. Human podoplanin was localized on the LEC surface by immunoelectron microscopy, and found to resist protease treatment used to dissociate cutaneous microvascular cells (reference 4; this study). These properties qualified podoplanin as useful marker for the separation of dermal LECs and BECs by FACS®.

In the past, several attempts have been made to obtain pure populations of bona fide LECs, for example by isolating cells from lymphatic vascular tumors (25, 26). Again, due to the lack of specific markers, the histogenetic origin of these expanded ECs could not be defined, or the isolated neoplastic ECs did not maintain a stable phenotype in culture. The triple fluorescence FACS® strategy used in this study allows for the first time the establishment and stable propagation of nontransformed, pure LECs and BECs. LECs were defined by the expression of podoplanin and CD34, and lack of CD45. Vice versa, BECs expressed CD34, but were devoid of podoplanin and CD45. These immunophenotypes directly relate to those of LECs and BECs in vivo. The podoplanin$^+$ and podoplanin$^-$ phenotype of LECs and BECs, respectively, were equally conserved after direct isolation of ECs (Materials and Methods, approach A) and following EC subset purification from bulk EC cultures (Materials and Methods, approach B). In the latter expansion cultures, compact islands of podoplanin$^+$ ECs were always surrounded by a lawn of podoplanin$^-$ ECs, and there was no apparent selection of one over the other subset. Similar to podoplanin, LYVE-1 remained stably expressed in cultured LECs for up to seven passages and was not induced in BECs. Vice versa, the antigen defined by mAb Pal-E was expressed in BECs but not in LECs. Common EC markers, such as CD31, VE-cadherin, UEA I reactivity, caveolin, vWF, and corresponding WP bodies, were observed in both LECs and BECs, though at somewhat different quantities. Thus, proteins that are exclusively expressed, or shared, by LECs or BECs in vivo remained unchanged during in vitro propagation of the isolated EC populations. Collectively, our studies on ex vivo isolated and in vitro propagated EC subsets strongly support that LECs and BECs represent two distinct and stable microvascular EC lineages.

Recently, VEGF-C was established as a lymphatic vessel–specific growth factor as evidenced by dermal lymphangioma-like vessel proliferation in mice that overexpress VEGF-C in the epidermis (27). Moreover, the induced expression of VEGF-C and -D in tumor cells caused massive intra-/peritumoral growth of lymphatic vessels and enhanced lymph node metastasis in mice (28–31). Here we show that VEGF-C mRNA and protein are produced by BECs, but not, or in minute quantities only, by LECs. Conversely, the receptor for VEGF-C, Flt-4, was almost exclusively expressed by LECs, rather than by BECs (Fig. 3, B and D). LECs produced three major Flt-4 isoforms, corresponding by MW to the mature form (~195 kD) of Flt-4 (15; Fig. 3 D), a nonglycosylated backbone (~140 kD), and the major precursor (~175 kD). A ~125 kD cleaved/processed COOH-terminal fragment of Flt-4 (15) was also detected on LECs, and in even higher levels on BECs (Fig. 3 D, and data not shown). Evidence was provided in this study, by different independent methods, that Flt-4 is expressed, though at low levels, by dermal BECs. The potential of BECs to express Flt-4 is further documented by pronounced Flt-4 expression on endothelia of tumor-associated blood vessels (12, 14). Furthermore, the weak Flt-4 expression of normal BECs (12) may have escaped detection by in situ labeling techniques used in previous studies. The other VEGF receptors, KDR and Flt-1, and the angiopoietin receptors Tie 1 and Tie 2 were detected in LECs and BECs at similar levels. These results raise the possibility that BECs use the VEGF-C-Flt-4 receptor system for unidirectional, interlineage communication with LECs. In vivo, the regeneration of lymphatics follows that of blood vessels with a significant delay, thought the reason for this has remained unexplained (2). Our data offer the appealing explanation that the blood vasculature has to reestablish before it directly induces proliferation of LECs and sprouting of new lymph vessels via the secretion of VEGF-C.

Do BECs and LECs form homotypic or also heterotypic cell contacts? Individually grown LECs and BECs formed conventional EC monolayers when grown to confluence. In mixed cultures that contained both EC types, LECs and BECs could not be distinguished by morphology, thus pretending their belonging to a single cell lineage. However, anti-podoplanin immunostaining revealed that LECs formed islands of homotypic cell aggregates. This homotypic association was even more evident when mixed cultures were grown to confluence, and EC bilayers formed that consisted of a lower layer of BECs and of an upper layer of LECs. This indicates specific mechanisms of homotypic recognition and formation of cell contacts, and presumably also different strength of cell-substrate adhesion. Also, signals elaborated by either cell type do not suffice to arrest growth of the other cell type.

Homotypic cell association was observed also when mixed EC populations were subjected to vascular "tube-formation" assays in Matrigel. LECs and BECs formed capillary "tubes" equally well when cultured separately. When fluorescence-tagged LECs and BECs were mixed in equal numbers and cocultured in Matrigel, continuous, strictly homotypic tubes emerged that were invariably closely asso-

ciated with each other, occasionally resembling helical doublets. This topographic behavior strikingly resembles the in vivo association of lymphatic and blood vessels in many tissues (1–3). A plausible explanation for this phenomenon could be that VEGF-C released from BECs "cross-talks" with its receptor Flt-4 that is primarily expressed on LECs.

While the molecular basis of this remarkable selectivity in cell–cell interaction remains to be established, our results show that cell contacts between LECs and those between BECs strikingly differ in the amount of junctional protein recruitment, and in the degree to which adjacent cell membranes were juxtaposed. LECs expressed less VE-cadherin, CD31, and catenins than BECs at junctional sites and formed rather narrow contact areas with neighboring cells. Nevertheless, LECs formed organized and close cell contacts that involved adherens, gap, and, even, tight junctions and were only poorly penetrated by exogenous soluble proteins. These elaborate and complex cellular interactions and junctions suggest a more stringent barrier function of LECs in lymphatic vessels than previously anticipated. Similar to BECs, LECs contain typical endothelial caveolae that mediate transcytotic transport across the endothelial barrier.

Lymphatic capillaries direct migratory APCs, i.e., dendritic cells (DCs), from the tissues toward the regional lymph nodes (32). It is still undecided whether LECs actively recruit tissue DCs into the lymphatic channels or merely provide a structural scaffold for continuous lymph fluid. The CC chemokine receptor 7 (CCR7) ligands SLC/CCL21 and MIP-3β/CCL19 were recently associated with the regulation of DC emigration from the tissues (33–36). Here we show that SLC/CCL21 is expressed in an activation-independent fashion by isolated LECs, but not by BECs and many other cell types. Moreover, >30% of this chemokine was secreted at the basolateral aspect of LECs while the inducible chemokine MIP-3α/CCL20 was secreted apically/luminally by BECs and LECs. The second known CCR7 ligand, CCL19, although found associated with afferent lymphatics by immunohistochemistry (37), was not secreted in significant amounts by either EC type whether stimulated or not. Thus, basolaterally/abluminally secreted SLC/CCL21 is a prime candidate for the recruitment of CCR7-expressing mature DCs from the interstitial spaces toward lymph vessels. LEC-derived SLC can also be of central importance for the dissemination of certain cancers. Melanoma and breast cancer cells, unlike their nontransformed counterparts, express functional CCR7 (38). Presumably, LECs actively control immune and tumor cell trafficking, using the similar ligand-receptor systems.

Mice with a deletion in the *Scya21a* gene (*plt*, paucity of lymph node T cell mice) fail to express CCL21 in lymphoid organs but express the *Scya21b* gene product SLC-Leu/CC21b in lymphatic ECs of nonlymphoid tissues (39). *plt* mice, in striking contrast to $CCR7^{-/-}$ mice, show normal delayed-type T cell responses (36, 40). It thus follows that LEC-derived rather than lymph node–expressed SLC is indispensable for proper DC homing to lymph nodes and, consecutively, T cell priming.

The fraction of SLC/CCL21 and MIP-3α/CCL20 that LECs secrete into the apical direction and thus presumably into the lumen of lymphatic capillaries will drain into regional nodes. As intradermally injected chemokines can be presented by ECs of high endothelial venules in lymph nodes (41), it is conceivable that LEC-derived CCL20 and CCL21 assist the recruitment of blood-borne $CCR6^{+}$ and $CCR7^{+}$ leukocytes into T cell zones of draining nodes. This would assign to LECs a novel immunoregulatory function for assuring optimal immune surveillance.

Taken together, stable EC subset-restricted gene expression and polarized secretion of function-related chemokines demonstrate that LECs and BECs belong to two different EC lineages. This is in agreement with the EC subtype-restricted importance of certain homeobox gene products, e.g., Prox-1, for the development of the lymphatic but not the blood vascular system (42). The availability of microvascular LECs will now allow the resolution of their genetic and functional programs, will help to uncover their contribution to the molecular pathogenesis of fatal conditions, such as cancer dissemination or transplant rejection, and, hopefully, will provide clues for the design of novel therapeutic strategies.

This work was supported by the Interdisciplinary Cooperation Project (ICP) Molecular Medicine, a program of the Austrian Ministry for Science (to D. Maurer and G. Stingl), by the Center of Molecular Medicine and the Austrian Academy of Sciences (to D. Maurer), and the Fonds zur Förderung der Wissenschaftlichen Forschung, SFB 05, Project 007; and EC Contract no. QLG1-2000-00619 (to D. Kerjaschki).

Submitted: 22 March 2001
Revised: 22 June 2001
Accepted: 18 July 2001

References

1. Skobe, M., and M. Detmar. 2000. Structure, function, and molecular control of the skin lymphatic system. *J. Invest. Dermatol. Symp. Proc.* 5:14–19.
2. Witte, M.H., D.L. Way, C.L. Witte, and M. Bernas. 1997. Lymphangiogenesis: mechanisms, significance, and clinical implication. *EXS.* 79:65–112.
3. Ryan, T.J. 1989. Structure and function of lymphatics. *J. Invest. Dermatol.* 93(Suppl.):18S–24S.
4. Breiteneder-Geleff, S., A. Soleiman, H. Kowalski, R. Horvat, G. Amann, E. Kriehuber, K. Diem, W. Weninger, E. Tschachler, K. Alitalo, and D. Kerjaschki. 1999. Angiosarcomas express mixed endothelial phenotypes of blood and lymphatic capillaries: podoplanin as a specific marker for lymphatic endothelium. *Am. J. Pathol.* 154:385–394.
5. Jaksits, S., E. Kriehuber, A.-S. Charbonnier, K. Rappersberger, G. Stingl, and D. Maurer. 1999. $CD34^{+}$ cell-derived $CD14^{+}$ precursor cells develop into Langerhans cells in a TGF-beta 1-dependent manner. *J. Immunol.* 163:4869–4877.
6. Sauter, B., D. Foedinger, B. Sterniczky, K. Wolff, and K. Rappersberger. 1998. Immunoelectron microscopic characterization of human dermal lymphatic microvascular endo-

thelial cells. Differential expression of CD31, CD34, and type IV collagen with lymphatic endothelial cells vs blood capillary endothelial cells in normal human skin, lymphangioma, and hemangioma in situ. *J. Histochem. Cytochem.* 46:165–176.
7. Erhard, H., F.J. Rietveld, E.B. Brocker, R.M. de Waal, and D.J. Ruiter. 1996. Phenotype of normal cutaneous microvasculature. Immunoelectron microscopic observations with emphasis on the differences between blood vessels and lymphatics. *J. Invest. Dermatol.* 106:135–140.
8. Chesney, J., M. Bacher, A. Bender, and R. Bucala. 1997. The peripheral blood fibrocyte is a potent antigen-presenting cell capable of priming naive T cells in situ. *Proc. Natl. Acad. Sci. USA.* 94:6307–6312.
9. Delia, D., M.G. Lampugnani, M. Resnati, E. Dejana, A. Aiello, E. Fontanella, D. Soligo, M.A. Pierotti, and M.F. Greaves. 1993. CD34 expression is regulated reciprocally with adhesion molecules in vascular endothelial cells in vitro. *Blood.* 81:1001–1008.
10. Banerji, S., J. Ni, S.X. Wang, S. Clasper, J. Su, R. Tammi, M. Jones, and D.G. Jackson. 1999. LYVE-1, a new homologue of the CD44 glycoprotein, is a lymph-specific receptor for hyaluronan. *J. Cell Biol.* 144:789–801.
11. Kaipainen, A., J. Korhonen, T. Mustonen, V.W. van Hinsbergh, G.H. Fang, D. Dumont, M. Breitman, and K. Alitalo. 1995. Expression of the fms-like tyrosine kinase 4 gene becomes restricted to lymphatic endothelium during development. *Proc. Natl. Acad. Sci. USA.* 92:3566–3570.
12. Valtola, R., P. Salven, P. Heikkila, J. Taipale, H. Joensuu, M. Rehn, T. Pihlajaniemi, H. Weich, R. deWaal, and K. Alitalo. 1999. VEGFR-3 and its ligand VEGF-C are associated with angiogenesis in breast cancer. *Am. J. Pathol.* 154:1381–1390.
13. Partanen, T.A., J. Arola, A. Saaristo, L. Jussila, A. Ora, M. Miettinen, S.A. Stacker, M.G. Achen, and K. Alitalo. 2000. VEGF-C and VEGF-D expression in neuroendocrine cells and their receptor, VEGFR-3, in fenestrated blood vessels in human tissues. *FASEB J.* 14:2087–2096.
14. Niki, T., S. Iba, T. Yamada, Y. Matsuno, B. Enholm, and S. Hirohashi. 2001. Expression of vascular endothelial growth factor receptor 3 in blood and lymphatic vessels of lung adenocarcinoma. *J. Pathol.* 193:450–457.
15. Pajusola, K., O. Aprelikova, G. Pelicci, H. Weich, L. Claesson-Welsh, and K. Alitalo. 1996. Signalling properties of FLT4, a proteolytically processed receptor tyrosine kinase related to two VEGF receptors. *Oncogene.* 9:3545–3555.
16. Kubota, Y., H.K. Kleinman, G.R. Martin, and T.J. Lawley. 1988. Role of laminin and basement membrane in the morphological differentiation of human endothelial cells into capillary-like structures. *J. Cell Biol.* 107:1589–1598.
17. Helmlinger, G., E. Endo, N. Ferrara, L. Hlatky, and R.K. Jain. 2000. Growth factors: formation of endothelial cell networks. *Nature.* 405:139–141.
18. Carmeliet, P., and R.K. Jain. 2000. Angiogenesis in cancer and other diseases. *Nature.* 407:249–257.
19. Yancopoulos, G.D., S. Davis, N.W. Gale, J.S. Rudge, S.J. Wiegand, and J. Holash. 2000. Vascular-specific growth factors and blood vessel formation. *Nature.* 407:242–248.
20. von Andrian, U.H., and C.R. Mackay. 2000. T-cell function and migration. Two sides of the same coin. *N. Engl. J. Med.* 343:1020–1034.
21. Breiteneder-Geleff, S., K. Matsui, A. Soleiman, P. Meraner, H. Poczewski, R. Kalt, G. Schaffner, and D. Kerjaschki. 1997. Podoplanin, a novel 43-kd membrane protein of glomerular epithelial cells, is down-regulated in puromycin nephrosis. *Am. J. Pathol.* 151:1141–1152.
22. Wetterwald, A., W. Hoffstetter, M.G. Cecchini, B. Lanske, C. Wagner, H. Fleisch, and M. Atkinson. 1996. Characterization and cloning of the E11 antigen, a marker expressed by rat osteoblasts and osteocytes. *Bone.* 18:125–132.
23. Rishi, A.K., M. Joyce-Brady, J. Fisher, L.G. Dobbs, J. Floros, J. VanderSpek, J.S. Brody, and M.C. Williams. 1995. Cloning, characterization, and development expression of a rat lung alveolar type I cell gene in embryonic endodermal and neural derivatives. *Dev. Biol.* 167:294–306.
24. Prevo, R., S. Banerji, D.J. Ferguson, S. Clasper, and D.G. Jackson. 2001. Mouse LYVE-1 is an endocytic receptor for hyaluronan in lymphatic endothelium. *J. Biol. Chem.* 276: 19420–19430.
25. Mancardi, S., G. Stanta, N. Dusetti, M. Bestagno, L. Jussila, M. Zweyer, G. Lunazzi, D. Dumont, K. Alitalo, and O.R. Burrone. 1999. Lymphatic endothelial tumors induced by intraperitoneal injection of incomplete Freund's adjuvant. *Exp. Cell Res.* 246:368–375.
26. Weninger, W., T.A. Partanen, S. Breiteneder-Geleff, C. Mayer, H. Kowalski, M. Mildner, J. Pammer, M. Stürzl, D. Kerjaschki, K. Alitalo, and E. Tschachler. 1999. Expression of vascular endothelial growth factor receptor-3 and podoplanin suggests a lymphatic endothelial cell origin of Kaposi's sarcoma tumor cells. *Lab. Invest.* 79:243–251.
27. Jeltsch, M., A. Kaipainen, V. Joukov, X. Meng, M. Lakso, H. Rauvala, M. Swartz, D. Fukumura, R.K. Jain, and K. Alitalo. 1997. Hyperplasia of lymphatic vessels in VEGF-C transgenic mice. *Science.* 276:1423–1425.
28. Mandriota, S.J., L. Jussila, M. Jeltsch, A. Compagni, R. Prevo, S. Banerji, J. Huarte, D. Baetens, R. Montesano, D.G. Jackson, et al. 2000. VEGF-C-mediated lymphangiogenesis promotes tumour metastasis. *J. Submicrosc. Cytol. Pathol.* 32:384. (Abstr.)
29. Skobe, M., T. Hawighorst, D.G. Jackson, R. Prevo, L. Janes, P. Velasco, L. Riccardi, K. Alitalo, K. Claffey, and M. Detmar. 2001. Induction of tumor lymphangiogenesis by VEGF-C promotes breast cancer metastasis. *Nat. Med.* 7:192–198.
30. Mandriota, S.J., L. Jussila, M. Jeltsch, A. Compagni, D. Baetens, R. Prevo, S. Banerji, J. Huarte, R. Montesano, D.G. Jackson, et al. 2001. Vascular endothelial growth factor-C-mediated lymphangiogenesis promotes tumour metastasis. *EMBO J.* 20:672–682.
31. Stacker, S.A., C. Caesar, M.E. Baldwin, G.E. Thornton, R.A. Williams, R. Prevo, D.G. Jackson, S.S. Nishikawa, H. Kubo, and M.G. Achen. 2001. VEGF-D promotes the metastatic spread of tumor cells via the lymphatics. *Nat. Med.* 7:186-191.
32. Lukas, M., H. Stössel, L. Hefel, S. Imamura, P. Fritsch, N.T. Sepp, G. Schuler, and N. Romani. 1996. Human cutaneous dendritic cells migrate through dermal lymphatic vessels in a skin organ culture model. *J. Invest. Dermatol.* 106:1293–1299.
33. Engeman, T.M., A.V. Gorbachev, R.P. Gladue, P.S. Heeger, and R.L. Fairchild. 2000. Inhibition of functional T cell priming and contact hypersensitivity responses by treatment with anti-secondary lymphoid chemokine antibody during hapten sensitization. *J. Immunol.* 164:5207–5214.
34. Gunn, M.D., S. Kyuwa, C. Tam, T. Kakiuchi, A. Matsuzawa, L.T. Williams, and H. Nakano. 1999. Mice lacking expression of secondary lymphoid organ chemokine have defects in lymphocyte homing and dendritic cell localization. *J. Exp. Med.* 189:451–460.

35. Robbiani, D.F., R.A. Finch, D. Jager, W.A. Muller, A.C. Sartorelli, and G.J. Randolph. 2000. The leukotriene C(4) transporter MRP1 regulates CCL19 (MIP-3β, ELC)-dependent mobilization of dendritic cells to lymph nodes. *Cell.* 103:757–768.
36. Förster, R., A. Schubel, D. Breitfeld, E. Kremmer, I. Renner-Muller, E. Wolf, and M. Lipp. 1999. CCR7 coordinates the primary immune response by establishing functional microenvironments in secondary lymphoid organs. *Cell.* 99:23–33.
37. Charbonnier, A.S., N. Kohrgruber, E. Kriehuber, G. Stingl, A. Rot, and D. Maurer. 1999. Macrophage inflammatory protein 3α is involved in the constitutive trafficking of epidermal Langerhans cells. *J. Exp. Med.* 190:1755–1768.
38. Muller, A., B. Homey, H. Soto, N. Ge, D. Catron, M.E. Buchanan, T. McClanahan, E. Murphy, W. Yuan, S.N. Wagner, et al. 2001. Involvement of chemokine receptors in breast cancer metastasis. *Nature.* 410:50–56.
39. Nakano, H., and M.D. Gunn. 2001. Gene duplications at the chemokine locus on mouse chromosome 4: multiple strain-specific haplotypes and the deletion of secondary lymphoid-organ chemokine and EBI-1 ligand chemokine genes in the plt mutation. *J. Immunol.* 166:361–369.
40. Mori, S., H. Nakano, K. Aritomi, C.-R. Wang, M.D. Gunn, and T. Kakiuchi. 2001. Mice lacking expression of the chemokines CCL21-Ser and CCL19 (*plt* mice) demonstrate delayed but enhanced T cell immune responses. *J. Exp. Med.* 193:207–218.
41. Stein, J.V., A. Rot, Y. Luo, M. Narasimhaswamy, H. Nakano, M.D. Gunn, A. Matsuzawa, E.J. Quackenbush, M.E. Dorf, and U.H. von Andrian. 2000. The CC chemokine thymus-derived chemotactic agent 4 (TCA-4, secondary lymphoid tissue chemokine, 6Ckine, exodus-2) triggers lymphocyte function–associated antigen 1–mediated arrest of rolling T lymphocytes in peripheral lymph node high endothelial venules. *J. Exp. Med.* 191:61–76.
42. Wigle, J.T., and G. Oliver. 1999. Prox1 function is required for the development of the murine lymphatic system. *Cell.* 98:769–778.